Theoretical and Experimental Studies on Elementary Reactions in Living Radical Polymerization via Organic Amine Catalysis

Atsushi Goto,[1]* *Shohei Sanada,*[2] *Lin Lei,*[3] *Kenji Hori*[2]*

[1]Division of Chemistry and Biological Chemistry, School of Physical and Mathematical Sciences, Nanyang Technological University, 21 Nanyang Link, 637371 Singapore

[2]Graduate School of Science and Engineering, Yamaguchi University, 2-16-1 Tokiwadai, Ube, Yamaguchi 755-8611, Japan

[3]Key Laboratory of Synthetic and Natural Functional Molecule Chemistry of Ministry of Education, College of Chemistry and Materials Science, Northwest University, Xi'an, Shaanxi 710069, China

KEYWORDS: transition state quantum calculation, living radical polymerization, organic catalysis

ABSTRACT: The reaction mechanism of living radical polymerization using organic catalysts, a reversible complexation mediated polymerization (RCMP), was studied using both theoretical calculations and experiments. The studied catalysts are tetramethyl guanidine (TMG), triethylamine (TEA), and thiophene. Methyl 2-iodoisoburylate (MMA–I) was used as the low-molar-mass model of the dormant species (alkyl iodide) of poly(methyl methacrylate) iodide (PMMA-I). For the reaction of MMA-I with TEA to generate MMA$^\bullet$ and $^\bullet$I-TEA radicals (activation process), the Gibbs activation free energy for the inner sphere electron transfer mechanism was calculated to be 39.7 kcal mol^{-1}, while the observed one was 25.1 kcal mol^{-1}. This difference of the energies suggests that the present RCMP proceeds via the outer sphere electron transfer mechanism, i.e., single-electron transfer (SET) reaction from TEA to MMA-I to generate MMA$^\bullet$ and $^\bullet$I-TEA radicals. The mechanism of the deactivation process of MMA$^\bullet$ to generate MMA-I was also theoretically studied. For the studied three catalysts, the theoretical results reasonably elucidated the experimentally observed polymerization behaviors.

INTRODUCTION

Much attention has been focused on living radical polymerizations (LRP) as a useful technique for preparing well-defined polymers with narrow molecular weight distributions.[1-5] LRP is based on the reversible activation of a dormant species (P–X) to a propagating radical ($P^\bullet$) (Scheme 1a), where P denotes a polymer. A sufficiently large number of activation-deactivation cycles are required to achieve low polydispersity.[6]

Goto et al. developed new LRP systems using iodine as a capping agent (X) and organic molecules as catalysts. These systems consist of a reversible chain transfer catalyzed polymerization (RTCP)[7] and a reversible complexation mediated polymerization (RCMP),[8-11] the latter of which is the focus of the present paper. An attractive feature of RCMP is that no special capping agents or metals are used. In addition, the catalysts are inexpensive, relatively non-toxic, easy to handle, and amenable to a wide range of monomers and polymer architectures. RCMP can be a useful methodology for a variety of applications.

Scheme 1. Reversible activation: (a) General scheme, (b) RCMP, and (c) ATRP.

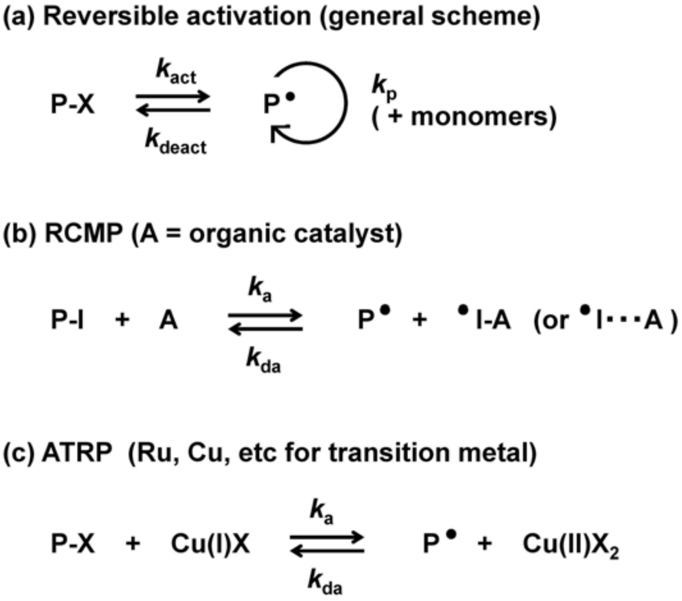

Catalysts for RCMP include organic amines such as tributylamine (TBA),[8] organic salts such as tetrabutylammonium iodide,[9] and organic superbases such as tetramethyl guanidine (TMG)[10] (Figure 1). RCMP is based on the reversible reaction between a dormant species (P–I) with a catalyst (A) to generate $P^\bullet$ and a catalyst-iodine complex ($^\bullet$I–A) (Scheme 1b). The iodine-catalyst bond in $^\bullet$I–A may not be a covalent or ionic bond but a coordination bond. For simplicity for discussions, the complex in any form will be written as $^\bullet$I–A in this paper.

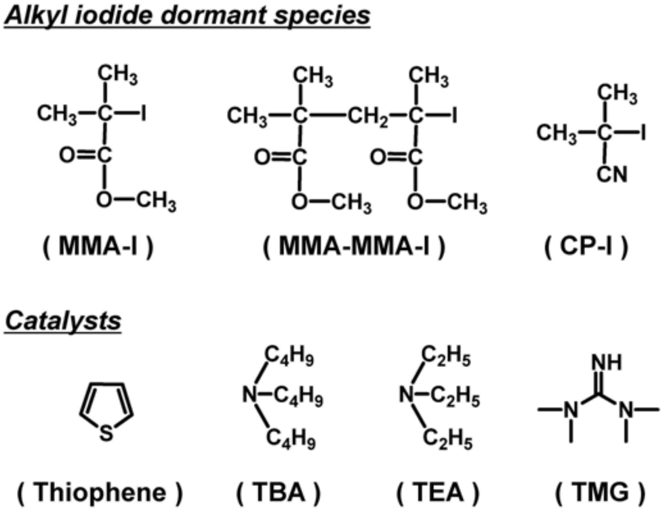

Figure 1. Structures of studied dormant species and catalysts.

Mechanistically, the background of RCMP is an atom transfer radical polymerization (ATRP) using halogens as the capping agents and transition metal compounds such as Cu(I)X as the activator catalysts (Scheme 1c).[2,3] Cu(I)X reversibly activates P–X to generate $P^\bullet$ and Cu(II)X_2. This is a redox reaction of the metal catalyst. RCMP can use organic molecules as catalysts instead of metal complexes. The polymerization involves a coordination reaction, which involves a relatively weak interaction between organic catalysts and iodine. This reaction allows for a variety of organic molecules to be used as catalysts, even though these organic molecules have no or weak redox abilities. The degree of the electron transfer from these organic catalysts to iodine ranges in different degrees from full (redox), partial (coordination) to nearly no transfer, depending on nature of catalysts. As RCMP is not a coordination polymerization but a radical polymerization, the term of coordination is used for interaction between organic catalysts and iodine in this paper. The propagating species in RCMP is a free radical.

In the literature, the reaction of an alkyl halide with an amine to generate an alkyl radical has been studied in organic chemistry.[12] In all cases, the reaction has been described as irreversible. We use a reversible reaction, which is new in chemistry, so that the mechanistic details of the reaction are not clear.

Theoretical calculation is a powerful tool for describing and understanding reaction mechanisms. The transition state (TS) calculation is very useful for probing the elementary reactions involved and visualizing how reactions proceed.[13-15] It is also useful for evaluating the reactivity of reactants and obtaining guidelines for the design of new efficient reactants.

In the present work, we applied theoretical calculations, which are compared with experimental results, to clarify the mechanisms and to evaluate reaction free energies of elementary reactions involved in RCMP. Figure 1 shows dormant species and catalysts used in the present study. We examined methyl 2-iodoisoburylate (MMA–I), which is a low-molar-mass model of a polymer, i.e., poly(methyl methacrylate) iodide (PMMA–I), as a dormant species. Triethylamine (TEA) is a representative RCMP catalyst and is structurally similar to TBA. Thus, we first examined TEA theoretically to elucidate mechanistic details of elementary reactions. TEA with ethyl groups was studied instead of TBA with heavier butyl groups for the simplicity of calculations for radicals. We then systematically studied thiophene and TMG, which are an ineffective and a highly effective catalyst, respectively, to discuss their structure-reactivity relationships. For this discussion, we compared theoretical energy profiles with experimental observations for polymerization reactions. The knowledge gained from this study will provide useful guidelines for designing efficient RCMP catalysts.

DEFINITION OF ELEMENTARY REACTIONS

Scheme 2 summarizes the elementary reactions involved in RCMP. In the present paper, we mainly discuss Reactions 1-5 and also provide some additional discussion of Reactions a1, a2, and a3. The k_m denotes the rate constant of reaction m. ΔG_m and $\Delta G_\mathrm{m}^{\ddagger}$ denote Gibbs free energy and Gibbs activation free energy of Reaction m, respectively.

Activation reaction. Reaction 1 is the reaction which produces active propagating species $\mathrm{P}^\bullet$. P–I reacts with A to generate $\mathrm{P}^\bullet$ and $^\bullet\mathrm{I}$–A, as mentioned above. This is the key reaction in RCMP. Highly efficient catalysts should have large activation rate constants k_1.

Scheme 2. Elementary Reactions Involved in RCMP.

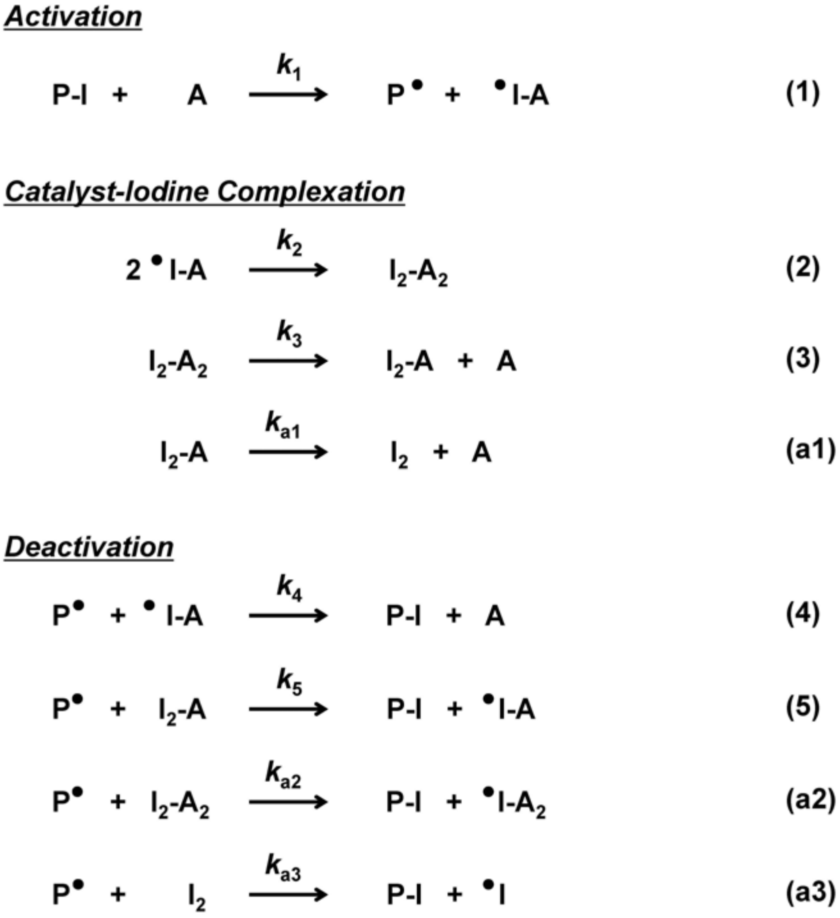

Iodine-Catalyst Complexation. The $^\bullet\mathrm{I}$–A radical generated in Reaction 1 is unstable so that it can easily recombine with another $^\bullet\mathrm{I}$–A radical to generate a complex consisting of an iodine molecule and two catalysts (I_2–A_2) (Reaction 2).[16] The I_2–A_2 molecule can release one of the catalyst molecules to form a complex I_2–A (Reaction 3).[17] This I_2–A complex was calculated to be energetically more favorable than I_2–A_2, as will be discussed later. Reaction a1 may successively proceed with releasing the second catalyst molecule from I_2-A to generate a free iodine molecule (I_2).[17] Although the reaction is reversible, its equilibrium is more shifted to I_2–A rather than to I_2, as will be discussed later. Thus, I_2–A is predominantly accumulated through Reactions 2 and 3.

It is possible to consider that I_2–A_2 takes an iodonium-salt-like structure such as $(A_2I)^+I^-$ so that the geometry of $(TEA_2I)^+I^-$ was optimized (Supporting Information). The salt structure was calculated to be less stable by 5.0 kcal/mol than its neutral form of TEA_2–I_2. In the present study, therefore, the salt-like structure was not considered in the reaction mechanism.

Deactivation process. The $P^\bullet$ radical reacts with the $^\bullet$I–A radical to form P-I and A (Reaction 4). This radical coupling should be a diffusion rate-controlling reaction. The $P^\bullet$ radical can also react with I_2–A_2, I_2–A, and I_2 molecules that are generated thorough the iodine-catalyst complexation mentioned above (Reactions 2, 3, and a1, respectively). Of the three species, I_2–A is predominantly accumulated, as suggested above. Thus, it is the most important to take Reaction 5 into account. Additional reactions to consider are Reactions a2 and a3, in which $P^\bullet$ reacts with I_2–A_2 and I_2, respectively. Reaction a3 is well known to be a nearly diffusion rate-controlling reaction[18] and hence can be important when the concentration of I_2 is sufficiently high in the reaction mixture.

THEORETICAL CALCULATION

All the calculations were carried out using the Gaussian 09 program.[19] Geometry optimizations and free energy profiles were calculated with the MP2 method. The LANL2DZ basis set was used for I (iodine), where the effective core potentials (ECPs) were employed to replace core electrons. For C, O, N, S and H atoms, the 6-31G(d) basis sets were employed (BAS-I). We confirmed that neither reactants nor products had imaginary frequencies in equilibrium structures and each transition state had only one imaginary frequency.

In order to obtain better energy profiles, MP2 energies were also calculated using better basis sets such as 6-311++G(2d) for I and 6-311++G(d,p) for the other atoms (BAS-II). Thermodynamic cycle[13,20] was applied to calculate free energy differences including solvent effects which were calculated using the SMD universal solvation model. The dielectric constant (ε = 6.25) of acetic acid was used instead of that of MMA (ε = 6.3) since the Gaussian09 program does not include that of MMA.

To confirm the validity of theoretical calculations, the activation free energy $\Delta G_p^{\ddagger}$ of a well-established reaction, i.e., propagation of the polymer radical PMMA$^{\bullet}$ to MMA, was calculated and compared with an experimentally obtained value, i.e., $\Delta G_{p}^{\ddagger}{}_{obs}$ = 15.3 kcal mol^{-1} of IUPAC recommended value.[21] The propagation rate constant (k_p) is about 16 times larger for a monomeric radical MMA$^{\bullet}$ (14000 M^{-1} s^{-1})[22] than a polymeric radical PMMA$^{\bullet}$ (840 M^{-1} s^{-1}) at 70 °C. The activation free energy for the monomeric MMA$^{\bullet}$ should be smaller by 1.8 kcal mol^{-1} than that of the polymeric PMMA$^{\bullet}$, and hence the $\Delta G_{p}^{\ddagger}{}_{obs}$ for the monomeric MMA$^{\bullet}$ is estimated to be 13.5 kcal mol^{-1}. Therefore, we have to remind this difference. The $\Delta G_{p}^{\ddagger}{}_{cal}$ value for the monomeric MMA$^{\bullet}$ to be 16.3 kcal mol^{-1}, which is larger by 2.8 kcal mol^{-1} than the experimental one. We have to remind such differences for free energy profiles for further discussions. The accuracy of the calculation may slightly be changed when heavy atoms such as iodine are involved in the reactions.

RESULTS AND DISCUSSION

Detailed Mechanism of Reaction 1 (Activation). We theoretically studied Reaction 1, using the monomeric model alkyl iodide MMA–I with TEA, TMG, and thiophene as the catalysts. There are two candidates as the reaction mechanisms. One proceeds via an iodine-bridged transition state in ATRP (inner sphere electron transfer) (Scheme 3a).[2,23] In this mechanism, the C-I bond homolytically breaks. The other involves a single electron transfer (SET) to form kinetically important intermediates, i.e., a donor cation ($A^{+\bullet}$) and an accepter anion ($P–I^{-\bullet}$) radicals in SET-LRP (outer sphere electron transfer) (Scheme 3b).[4] The $P–I^{-\bullet}$ radical heterolytically breaks to generate the $P^{\bullet}$ radical and the I^{-} anion, followed by the formation of the $^{\bullet}I–A$ radical.

Scheme 3. Possible Paths of Reaction 1.

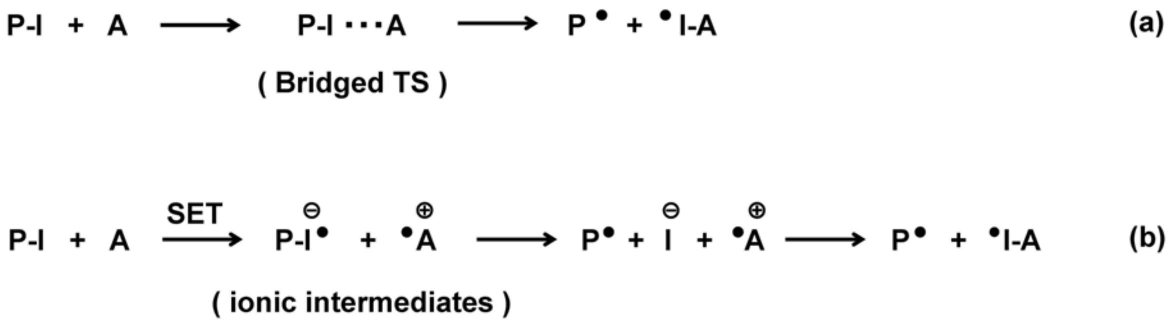

Figure 2 displays optimized structures for the bridged TS path with TEA. The C-I length of the reactant MMA-I was calculated to be 2.197 Å, and this C-I bond is elongated to 3.336 Å in the bridged TS. The N-I distance of the product $^{\bullet}I–TEA$ is rather long (2.765 Å) and thus this N-I bond should be weak.

As electronic and structural properties of the $^{\bullet}I–A$ radical are interesting since the reversibility of the reaction depends on its stability. Figure 3 depicts the calculated Mulliken charges and N-I or S-I distances in the $^{\bullet}I–A$ radicals with A = TEA, TMG, and thiophene. In the case of TEA, the Mulliken charge of the TEA fragment was partially positive (δ +0.16), and that of the iodine moiety was negative to the same extent. The TMG (δ +0.09) and thiophene (δ +0.11) fragments were also positively charged. These charge distributions indicate that only partial charge-transfer occurs from the catalyst to the iodine through the coordination of A to •I.

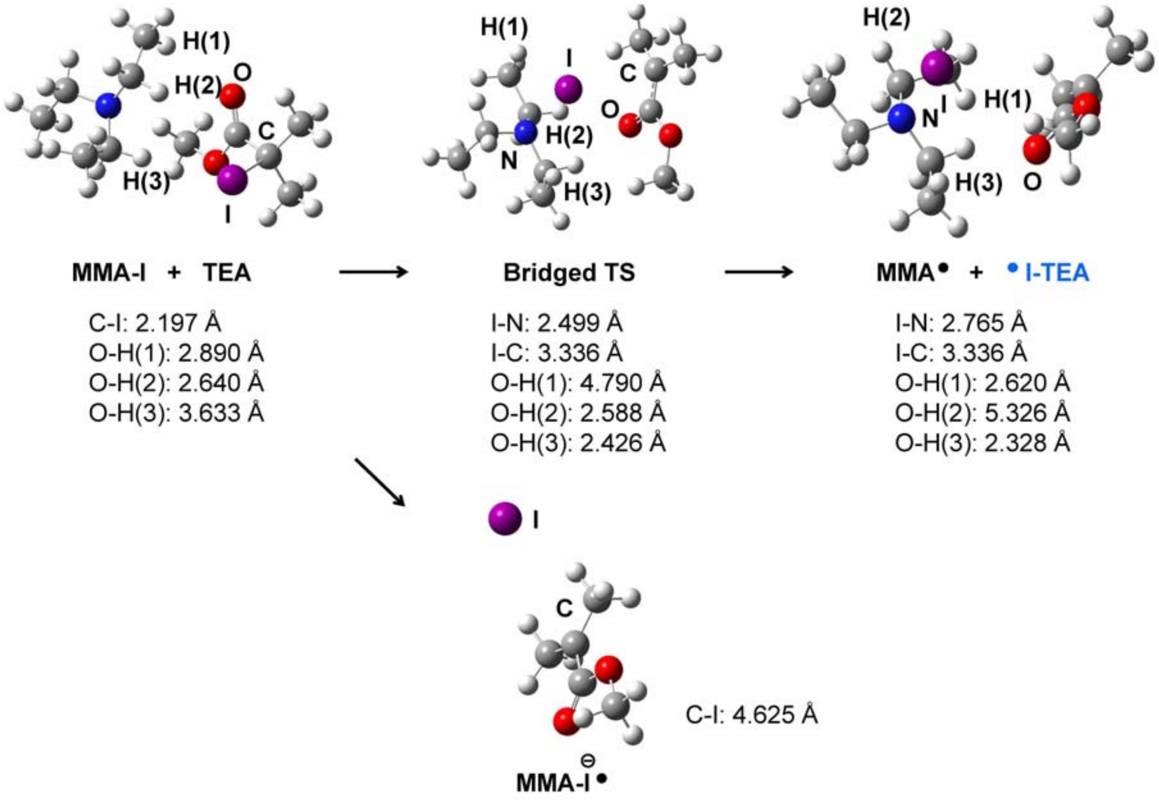

Figure 2. Optimized Structures for the reaction pathways via bridged TS and SET proposed in Scheme 3.

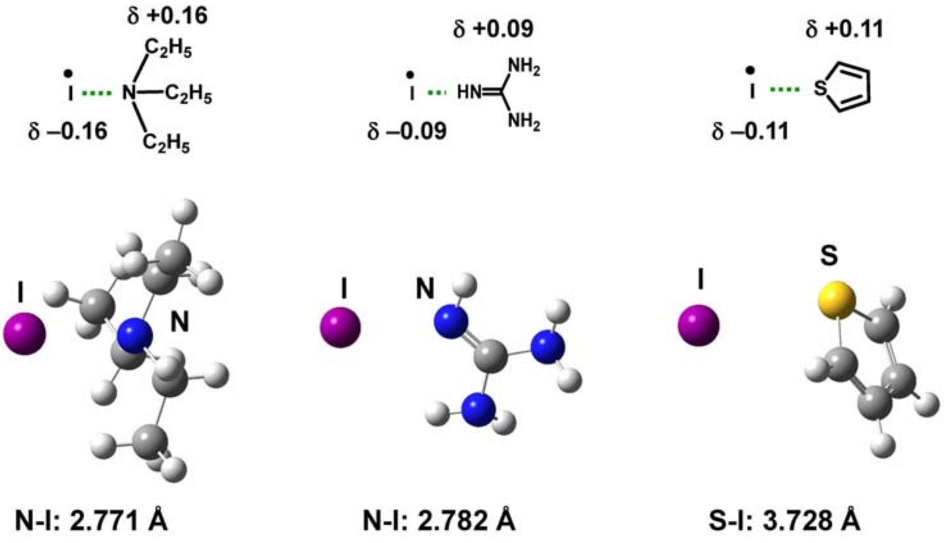

Figure 3. Structures and Mulliken charges of •I-A with A = TEA, TMG, and Thiophene.

The activation free energy $\Delta G_1^{\ddagger}$(BT) calculated for the bridged TS with TEA in MMA as solvent was calculated to be 39.7 kcal mol^{-1}. We have to remind that the calculated energy for the propagation reaction is consistent with the observed one within ~3 kcal mol^{-1}. The theory of absolute reaction rates indicates that this energy corresponds to a rate constant as small as 10^{-15} M^{-1} s^{-1} at a typical polymerization temperature 70 °C. This $\Delta G_1^{\ddagger}$(BT) value is too large for Reaction 1 to proceed via the bridged TS path under a reasonable rate (Scheme 3a).

Experimental $\Delta G_{1}^{\ddagger}{}_{\mathrm{obs}}$ Value of Reaction 1 Using TBA. For comparison of the theoretical result with an observed one, the rate constant k_1 of the polymeric PMMA–I with TBA catalyst in MMA medium (solvent) was experimentally measured at several temperatures (70–100 °C) using the method described in Supporting Information.[8,24] Figure 4 shows an Eyring plot using the obtained k_1 value.

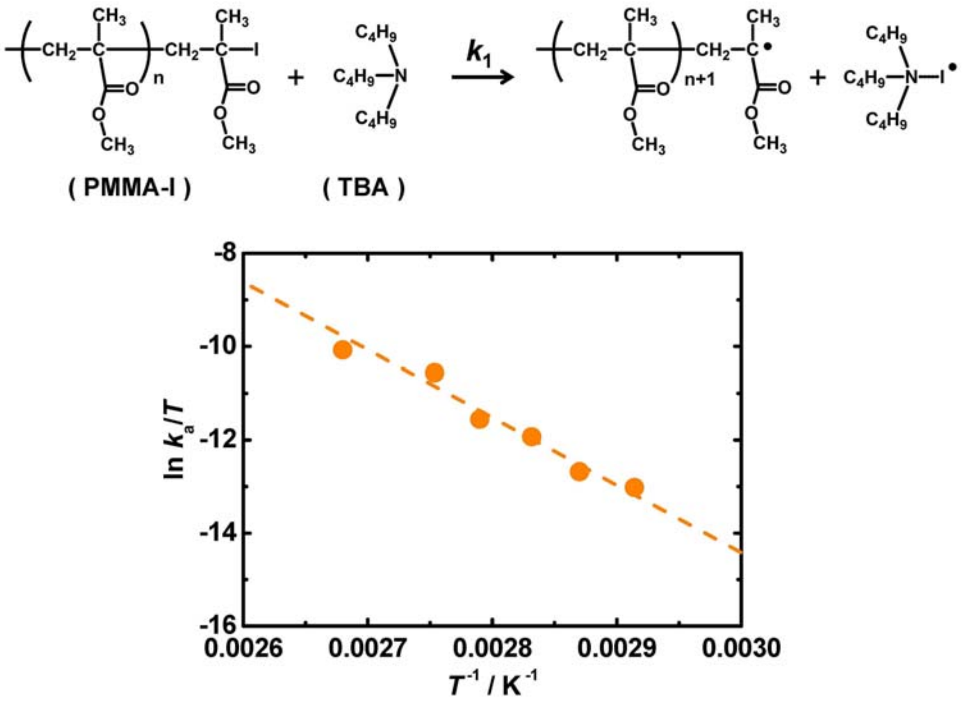

Figure 4. The Eyring plot of k_1 for polymeric PMMA–I with TBA in MMA monomer.

The activation enthalpy ($\Delta H_1^{\ddagger}$) and entropy ($\Delta S_1^{\ddagger}$) were observed to be 27.3 kcal mol^{-1} and 6.6 cal mol^{-1} K^{-1}, respectively, and, therefore, the observed activation free energy $\Delta G_1^{\ddagger}{}_{\mathrm{obs}}$ was 25.1 kcal mol^{-1} at 70 °C. This $\Delta G_1^{\ddagger}{}_{\mathrm{obs}}$ values is much smaller by 14.6 kcal mol^{-1} than the calculated $\Delta G_1^{\ddagger}$(BT) of 39.7 kcal mol^{-1}. This large difference again indicates that the bridged TS path (Scheme 3a) is not plausible for Reaction 1. Therefore, the observed $\Delta G_1^{\ddagger}{}_{\mathrm{obs}}$ value is likely to correspond to that for the SET process.

Because it is very difficult to optimize the structure of an intermediate for the SET mechanism (Scheme 3b), the cation $A^{+\bullet}$ and the anion P-I$^{-\bullet}$ radicals were optimized separately. The calculation suggested that the C-I bond of the P–I$^{-\bullet}$ anion spontaneously breaks to form P$^{\bullet}$ and I^{-} since the C-I length in the optimized anion P-I$^{-\bullet}$ radical was calculated to be as long as 4.625 Å (Figure 2).

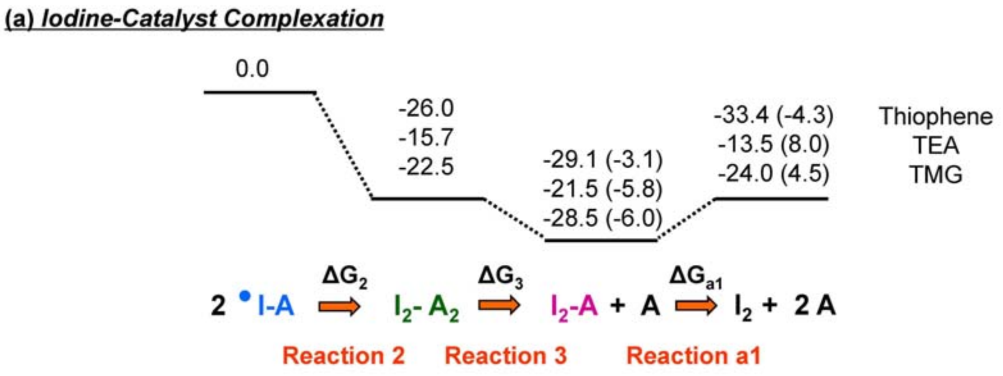
(a) *Iodine-Catalyst Complexation*

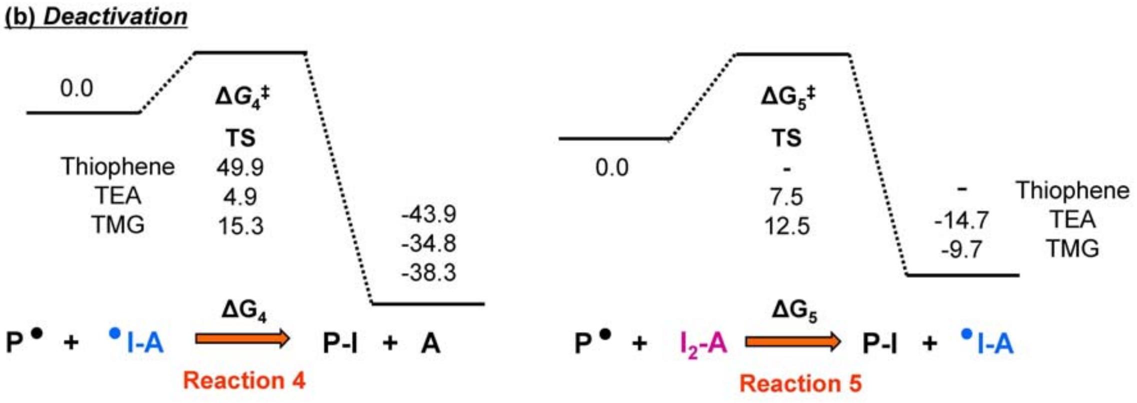
(b) *Deactivation*

Figure 5. Free energy profile of reactions 2-5 and a1 for MMA-I with the three catalysts in kcal/mol. Values in parentheses are energies relative to the previous position.

Reactions 2 and 3 of TEA (Iodine-Catalyst Complexation). Figure 5 summarizes energy profiles of Reactions 2-5 and a1. As the ΔG_2 value for TEA was calculated to be −15.7 kcal mol^{-1}, Reaction 2 proceed exothermically so that the reaction of the two $^{\bullet}$I–A radicals results in readily forming I_2–A_2 (Reaction 2). I_2–A_2 subsequently releases one catalyst molecule to generate I_2–A since Reaction 3 is also exothermic by 5.8 kcal mol^{-1}. On the other hand, Reaction a1, which releases the second catalyst from I_2–A to generate I_2 and A, is endothermic (ΔG_{a1} = 8.0 kcal mol^{-1}). These results indicate that among the possible four deactivators ($^{\bullet}$I–A, I_2–A_2, I_2–A, and I_2), I_2–A is predominantly accumulated during the polymerization.

Reactions 4 and 5 of TEA (Deactivation). As discussed above, the $P^{\bullet}$ and $^{\bullet}$I–A radicals are produced via the SET reaction with the energy barrier of $\Delta G_1{}^{\ddagger}{}_{obs}$ = 25.1 kcal mol^{-1} for TBA. The calculation showed that $P^{\bullet}$ + $^{\bullet}$I–A is less stable by ΔG_4 = –34.8 kcal mol^{-1} than P-I + A, as shown in Figure 5. The recombination of the two radicals, the deactivation reaction, was calculated to have a small energy barrier ($\Delta G_4{}^{\ddagger}$ = 4.9 kcal mol^{-1}) to release a relevant large stabilization (ΔG_4).

Reaction 5 plays an important role in the deactivation process due to the accumulation of I_2–A as mentioned above. The energy barrier $\Delta G_5{}^{\ddagger}$ is so small (7.5 kcal mol^{-1}) that the reaction can readily proceed. The reaction was calculated to be exothermic (ΔG_5 = −14.7 kcal mol^{-1}).

Other candidates for the deactivation are Reactions a2 and a3. Figure 6 summarizes the optimized structures for the deactivators, $^{\bullet}$I–A, I_2–A, and I_2–A_2 for Reaction 4, Reaction 5, and Reaction a2, respectively. The N-I-I-N fragment in the I_2–A_2 molecule (Reaction a2) takes a straight geometry so that two catalyst molecules sandwiches the I_2 fragment. This feature in geometry prevents $P^{\bullet}$ from approaching the internal I_2 moiety. The concentration of

I_2-A_2 is also not very high as discussed above, and thus Reaction a2 would be negligible. The significance of Reaction a3 depends on the concentration of I_2. The optimized I_2–A_2 structure for TMG also takes a similar geometry.

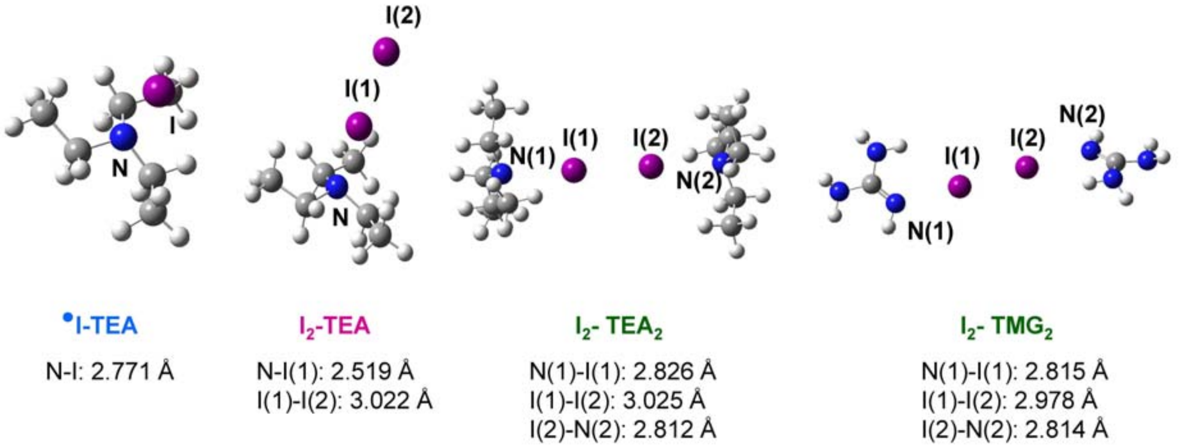

Figure 6. Geometry of iodine-TEA complexes.

In RCMP of MMA, tertiary amines (R_3N) such as TBA are used as catalysts in most cases.[8] When primary amines (RNH_2) are used, a side reaction, i.e., a substitution reaction of iodine of PMMA-I with RNH_2 to generate Polymer-NHR (chain-end transformation) can be significant. This side reaction is much faster for primary amines than secondary and tertiary amines[25] and is usually unimportant for tertiary amines.

Systematic Study of Different Catalysts in Experiments and Calculations. The key reaction in RCMP is Reaction 1 (activation) via the SET mechanism. Another key reaction is deactivation mainly via Reactions 4, 5, and a3. The balance of activation and deactivation reactions should be important for controlling the molecular weight and its distribution. The polymerization can proceed in three different manners. Our experimental results given below show these three different behaviors. Figure 7 shows experimental results of bulk polymerizations of MMA (100 eq) with 2-cyanopropyl iodide (CP–I) (1 eq) and three different catalysts (0.5 eq), i.e., thiophene, TBA and TMG at 70 °C.

The first case is thiophene. Activation (Reaction 1) is too slow. The polymerization did not proceed at all for 5 h, as shown in Figure 7a (open circle). (The polymerization did not proceed even for a long time 20 h.) The lone pair orbital of thiophene locates too low to take place the SET reaction. (In a reference experiment including only MMA and CP-I (with no catalyst), the polymerization (thermal polymerization initiated by thermal dissociation of CP-I) did not proceed.[8])

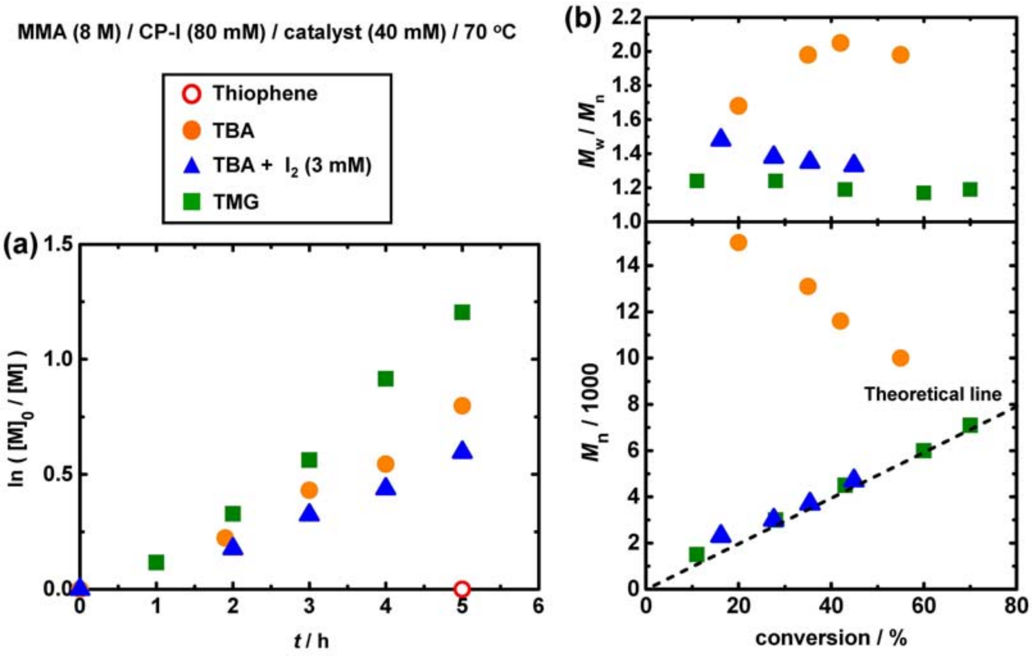

Figure 7. Plots of (a) ln($[M]_0$/[M]) vs t and (b) M_n and M_w/M_n vs conversion for the MMA/CP-I/catalyst systems (in bulk) (70 ^{o}C): $[MMA]_0$ = 8 M; $[CP\text{-}I]_0$ = 80 mM; $[catalyst]_0$ = 40 mM; $[I_2]_0$ = 0 or 3 mM. The symbols and catalysts are indicated in the figure.

The second case is TBA. Activation (Reaction 1) is fast, but deactivation is relatively slow. While the polymerization proceeded (filled circles), relatively high molecular weight species were generated at an early stage of polymerization (20% monomer conversion). Furthermore, neither molecular weights nor polydispersity of the polymer was controlled. In this system, the activation rate is fast enough, as experimentally observed ($\Delta G_1{}^{\ddagger}{}_{obs}$ = 25.1 kcal mol^{-1}). However, the deactivation rate is relatively slow, and too many monomers are added to $P^{\bullet}$ in one activation-deactivation cycle. The calculated small $\Delta G_4^{\ddagger}$ and $\Delta G_5^{\ddagger}$ values (4.9 and 7.5 kcal mol^{-1}) suggest that the rate constants k_4 and k_5 are rather large. Thus, the concentrations of the generated $^{\bullet}$I–A and I_2-A species must be too low. In such a system, addition of a small amount of I_2 is useful to increase the concentration of I_2-A which reacts $P^{\bullet}$ to effectively decrease the concentration of $P^{\bullet}$. In fact, this strategy worked well to control the molecular weights of polymers, as shown in Figure 7 (triangles). The polydispersity index (M_w/M_n) was small (approximately 1.4) for the conversion more than 30 % as expected. The addition of I_2 balances the activation reaction with the deactivation.

The third case is TMG. Activation (Reaction 1) is fast, and deactivation is also fast enough. As shown in Figure 7 (squares), the molecular weight of the polymer was almost proportional to the monomer conversion and well agreed with the theoretical value. The M_w/M_n value was small (approximately 1.3) from an early stage to the late stage (20% to 70% monomer conversion) of the polymerization. These results mean that both activation and deactivation rates are high enough to achieve low polydispersity.

The activation is likely to involve SET (as discussed above) and would be promoted with an increase of electron donating ability (basicity) of the catalyst. It is considered that the basicity increases is in the order of thiophene < TBA (base) (pK_b = 3.4) < TMG (superbase) (pK_b = –9.3).[26] (The pK_b values are those in water.) The deactivation rate depends on the concentrations and reaction rate constants of the four possible deactivators ($^{\bullet}$I–A, I_2–A_2, I_2–A, and I_2). Regarding the concentrations, I_2–A is predominantly accumulated for TBA, as discussed above. An interesting calculated result is that ΔG_{a1} for TMG (4.5 kcal mol^{-1}) is smaller than that of TEA (8.0 kcal mol^{-1}) as shown in Figure 5. This suggests that the generation of I_2 is not negligible and that both I_2-A and I_2 can be important deactivators in the TMG system. The $\Delta G_4^{\ddagger}$ (deactivation with $^{\bullet}$I–A) and $\Delta G_5^{\ddagger}$ (deactivation with I_2-A) values are small for both TEA and TMG. The observed fast deactivation in the TMG system would be explained by important involvement of I_2 as a deactivator (Reaction a3) as well as those of $^{\bullet}$I–A (Reaction 4) and I_2-A (Reaction 5).

CONCLUSIONS

Both the theoretical and the experimental results suggested that the activation to form the active radicals is likely to proceed via the SET path (Scheme 3b) rather than the bridged TS path (Scheme 3a) in the case of TEA. Through the iodine-catalyst complexation process (via Reactions 2, 3, and a1), I_2–A is predominantly accumulated among the possible four deactivators for TEA, both I_2–A and I_2 are accumulated for TMG, and I_2 is accumulated for thiophene. The deactivations with $^{\bullet}$I–A (Reaction 4) and I_2–A (Reaction 5) are exothermic for all studied catalysts. The $\Delta G_4^{\ddagger}$ and $\Delta G_5^{\ddagger}$ values for Reactions 5 and 4, respectively, are the smallest for TEA among the studied three catalysts.

ASSOCIATED CONTENT

Supporting Information

Experimental Section, Determination of k_1, Optimized Structure of $(TEA_2I)^+I^-$, and Theoretical Calculation Section. This material is available free of charge via the Internet at http://pubs.acs.org.

AUTHOR INFORMATION

Corresponding Author

*E-mail: agoto@ntu.edu.sg, kenji@yamaguchi-u.ac.jp

Notes

The authors declare no competing financial interest.

ACKNOWLEDGMENTS

This work was partly supported by Start-Up-Grant of Nanyang Technological University, and Research Funding of The Society of Iodine Science (SIS), Japan. The authors thank Ms. Taeko Oonuma and Dr. Tetsuya Noda at Mitsubishi Rayon Co., Ltd. for discussion.

REFERENCES

(1) (a) Matyjaszewski, K.; Sumerlin, B. S.; Tsarevsky, N. V.; Chiefari J. Controlled Radical Polymerization: Mechanisms. *ACS Symp. Ser.* **2015**, *1187*. (a) Matyjaszewski, K.; Sumerlin, B. S.; Tsarevsky, N. V.; Chiefari J. Controlled Radical Polymerization: Materials. *ACS Symp. Ser.* **2015**, *1188*. (c) Matyjaszewski, K.; Möller, M. *Polymer Science: A Comprehensive Reference*; Elsevier: Amsterdam, 2012. (d) Tsarevsky, N. V.; Sumerlin, B. S. *Fundamentals of Controlled/Living Radical Polymerization*; Royal Society of Chemistry: UK, 2013.

(2) Matyjaszewski, K.; Tsarevsky, N. V. Macromolecular Engineering by Atom Transfer Radical Polymerization. *J. Am. Chem. Soc.* **2014**, *136*, 6513-6533.

(3) Ouchi, M.; Terashima, T.; Sawamoto, M. Transition Metal-Catalyzed Living Radical Polymerization: Toward Perfection in Catalysis and Precision Polymer Synthesis. *Chem. Rev.* **2009**, *109*, 4963-5050.

(4) Zhang, N.; Samanta, S. R.; Rosen, B. M.; Percec, V. Single Electron Transfer in Radical Ion and Radical-Mediated Organic, Materials and Polymer Synthesis. *Chem. Rev.* **2014**, *114*, 5848-5958.

(5) (a) Nicolas, J.; Guillaneuf, Y.; Lefay, C.; Bertin, D.; Gigmes, D.; Charleux, B. Nitroxide-Mediated Polymerization. *Prog. Polym. Sci.* **2013**, *38*, 63–235. (b) David, G.; Boyer, C.; Tonnar, J.; Ameduri, B.; Lacroix-Desmazes, P.; Boutevin, B. Use of Iodocompounds in Radical Polymerization. *Chem. Rev.* **2006**, *106*, 3936-3962. (c) Keddie, D. J.; Moad, G.; Rizzardo, E.; Thang, S. H. RAFT Agent Design and Synthesis. *Macromolecules* **2012**, *45*, 5321-5342. (d) Yamago, S. Precision Polymer Synthesis by Degenerative Transfer Controlled/Living Radical Polymerization Using Organotellurium, Organostibine, and Organobismuthine Chain-Transfer Agents. *Chem. Rev.* **2009**, *109*, 5051-5068. (e) Zetterlund, P. B.; Kagawa, Y.; Okubo, M. Controlled/Living Radical Polymerization in Dispersed Systems. *Chem. Rev.* **2008**, *108*, 3747-3794. (f) Satoh, K.; Kamigaito, M. Stereospecific Living Radical Polymerization: Dual Control of Chain Length and Tacticity for Precision Polymer Synthesis. *Chem. Rev.* **2009**, *109*, 5120-5156. (g) Monteiro, M. J.; Cunningham, M. F. Polymer Nanoparticles via Living Radical Polymerization in Aqueous Dispersions: Design and Applications. *Macromolecules* **2012**, *45*, 4939-4957.

(6) For reviews on kinetic of LRP: (a) Fukuda, T. Fundamental Kinetic Aspects of Living Radical Polymerization and the Use of Gel Permeation Chromatography to Shed Light on Them. *J. Polym. Sci.: Part A: Polym. Chem.* **2004**, *42*, 4743-4755. (b) Fischer, H. The Persistent Radical Effect: A Principle for Selective Radical Reactions and Living Radical Polymerizations. *Chem. Rev.* **2001**, *101*, 3581-3618. (c) Goto, A.; Fukuda, T. Kinetics of Living Radical Polymerization. *Prog. Polym. Sci.* **2004**, *29*, 329-385.

(7) (a) Goto, A.; Zushi, H.; Hirai, N.; Wakada, T.; Tsujii, Y.; Fukuda, T. Living Radical Polymerizations with Germanium, Tin, and Phosphorus Catalysts - Reversible Chain Transfer Catalyzed Polymerizations (RTCPs). *J. Am. Chem. Soc.* **2007**, *129*, 13347-13354. (b) Goto, A.; Hirai, N.; Wakada, T.; Nagasawa, K.; Tsujii, Y.; Fukuda, T.

Living Radical Polymerization with Nitrogen Catalyst: Reversible Chain Transfer Catalyzed Polymerization with *N*-Iodosuccinimide. *Macromolecules* **2008**, *41*, 6261-6264. (c) Goto, A.; Hirai, N.; Nagasawa, K.; Tsujii, Y.; Fukuda, T.; Kaji, H. Phenols and Carbon Compounds as Efficient Organic Catalysts for Reversible Chain Transfer Catalyzed Living Radical Polymerization (RTCP). *Macromolecules* **2010**, *43*, 7971-7978. (d) Vana, P.; Goto, A. Kinetic Simulations of Reversible Chain Transfer Catalyzed Polymerization (RTCP): Guidelines to Optimum Molecular Weight Control. *Macromol. Theory Simul.* **2010**, *19*, 24-35. (e) Yorizane, M.; Nagasuga, T.; Kitayama, Y.; Tanaka, A.; Minami, H.; Goto, A.; Fukuda, T.; Okubo, M. Reversible Chain Transfer Catalyzed Polymerization (RTCP) of Methyl Methacrylate with Nitrogen Catalyst in an Aqueous Microsuspension System. *Macromolecules*, **2010**, 43, 8703-8705.

(8) Goto, A.; Suzuki, T.; Ohfuji, H.; Tanishima, M.; Fukuda, T.; Tsujii, Y.; Kaji, H. Reversible Complexation Mediated Living Radical Polymerization (RCMP) Using Organic Catalysts. *Macromolecules* **2011**, *44*, 8709-8715.

(9) Goto, A.; Ohtsuki, A.; Ohfuji, H.; Tanishima, M.; Kaji, H. Reversible Generation of a Carbon-Centered Radical from Alkyl Iodide Using Organic Salts and Their Application as Organic Catalysts in Living Radical Polymerization. *J. Am. Chem. Soc.* **2013**, *135*, 11131-11139.

(10) Lei, L.; Tanishima, M.; Goto, A.; Kaji, H. Living Radical Polymerization via Organic Superbase Catalysis. *Polymers* **2014**, *6*, 860-872.

(11) (a) Ohtsuki, A.; Goto, A.; Kaji, H. Visible-Light-Induced Reversible Complexation Mediated Living Radical Polymerization of Methacrylates with Organic Catalysts. *Macromolecules* **2013**, *46*, 96-102. (b) Lei, L.; Tanishima, M.; Goto, A.; Kaji, H.; Yamaguchi, Y.; Komatsu, H.; Jitsukawa, T.; Miyamoto, M. Systematic Study on Alkyl

Iodide Initiators in Living Radical Polymerization with Organic Catalysts. *Macromolecules* **2014**, *47*, 6610-6618. (c) Ohtsuki, A.; Lei, L.; Tanishima, M.; Goto, A.; Kaji, H. Photocontrolled Organocatalyzed Living Radical Polymerization Feasible over a Wide Range of Wavelengths. *J. Am. Chem. Soc.* **2015**, *137*, 5610-5617.

(12) (a) Stevenson, D. P.; Coppinger, G. M. Solvent Effects on (n → σ*) Transitions; Complex Formation between Amines and Halomethanes. *J. Am. Chem. Soc.* **1962**, *84*, 149-152. (b) Lautenberger, W. J.; Jones, E. N.; Miller, J. G. Reaction of Amines with Haloalkanes. I. Photochemical Reaction of Butylamine with Carbon Teterachloride. *J. Am. Chem. Soc.* **1968**, *90*, 1110-1115. (c) Ishibashi, H.: Haruki, S.; Uchiyama, M.; Tamura, O.; Matsuo, J. Radical Cyclizations in 1,4-Dimethylpiperazine. *Tetrahedron Lett.* **2006**, *47*, 6263-6266.

(13) Hori, K.; Sadatomi, H.; Miyamoto, A.; Kuroda, T.; Sumimoto, M.; Yamamoto, H. Towards the Development of Synthetic Routes Using Theoretical Calculations: An Application of In Silico Screening to 2,6-Dimethylchroman-4-one. *Molecule*, **2010**, 15, 8289-8304.

(14) Kaweetirawatt, T.; Yamaguchi, T.; Hayashiyama, S.; Sumimoto, M.; Kamimura, A.; Hori, K. Nylon 6 Depolymerization in Supercritical Alcohols Studied by the QM/MC/FEP Method. *RSC Advances*, **2012**, 2, 8402–8409.

(15) Sumimoto, M.; Kuroda, T.; Yokogawa, D.; Yamamoto, H.; Hori, K. Theoretical Study on a New Active Species for the Pd(II)-Catalyzed Mizoroki-Heck Reaction. *J. Organomet. Chem.*, **2012**, 710, 26-35.

(16) For the combination of two free $I^\bullet$s (not $I^\bullet$/amine complexes) to generate an iodine molecule I_2, (a) Rosman, H.; Noyes, R. M. Rate Constants for Combination of Iodine Atoms in Inert Solvents. *J. Am. Chem. Soc.* **1958**, *80*, 2410-2415. (b) Lacroix-

Desmazes, P.; Tonnar, J.; Boutevin, B. Reverse Iodine Transfer Polymerization (RITP) in Emulsion. *Macromol. Symp.* **2007**, *248*, 150-157.

(17) (a) Wan, J. K. S.; Pitts, J. N. A Spectroscopic Investigation of the Reaction between Iodine and Cycloproplyamine. *Tetrahedron Lett.* **1964**, *44*, 3245-3250. (b) Yada, H.; Tanaka, J.; Nagakura, S. Charge-Transfer Complexes between Iodine and Various Aliphatic Amines. *Bull. Chem. Soc. Jpn.* **1960**, *33*, 1660-1667. (c) Schmulbach, C. D.; Hart, D. M. Molecular Addition Compounds of Amines and Iodine. Evidence for the Existence of a 2:1 Triethylamine-Iodine Complex. *J. Am. Chem. Soc.* **1964**, *86*, 2347-2351. (d) Halpern, A. M.; Weiss, K. Intramolecular Perturbation Effects in Diamine-Iodine Charge-Transfer Complexes. *J. Am. Chem. Soc.* **1968**, *90*, 6297-6302.

(18) (a) Foldiak, G.; Schuler, R. H. Rate Constants for Scavenging of Radicals by Iodine. *J. Phys. Chem.* **1978**, *82*, 2756-2757. (b) Lacroix-Desmazes, P.; Severac, R.; Boutevin, B. Reverse Iodine Transfer Polymerization of Methyl Acrylate and *n*-Butyl Acrylate. *Macromolecules* **2005**, *38*, 6299-6309.

(19) Gaussian 09, Frisch, M. J.; Trucks, G. W.; Schlegel, H. B.; Scuseria, G. E.; Robb, M. A.; Cheeseman, J. R.; Scalmani, G.; Barone, V.; Mennucci, B.; Petersson, G. A.; Nakatsuji, H.; Caricato, M.; Li, X.; Hratchian, H. P.; Izmaylov, A. F.; Bloino, J.; Zheng, G.; Sonnenberg, J. L.; Hada, M.; Ehara, M.; Toyota, K.; Fukuda, R.; Hasegawa, J.; Ishida, M.; Nakajima, T.; Honda, Y.; Kitao, O.; Nakai, H.; Vreven, T.; Montgomery, Jr., J. A.; Peralta, J. E.; Ogliaro, F.; Bearpark, M.; Heyd, J. J.; Brothers, E.; Kudin, K. N.; Staroverov, V. N.; Kobayashi, R.; Normand, J.; Raghavachari, K.; Rendell, A.; Burant, J. C.; Iyengar, S. S.; Tomasi, J.; Cossi, M.; Rega, N.; Millam, J. M.; Klene, M.; Knox, J. E.; Cross, J. B.; Bakken, V.; Adamo, C.; Jaramillo, J.; Gomperts, R.; Stratmann, R. E.; Yazyev, O.; Austin, A. J.; Cammi, R.; Pomelli, C.; Ochterski, J. W.; Martin, R. L.;

Morokuma, K.; Zakrzewski, V. G.; Voth, G. A.; Salvador, P.; Dannenberg, J. J.; Dapprich, S.; Daniels, A. D.; Farkas, Ö.; Foresman, J. B.; Ortiz, J. V.; Cioslowski, J.; Fox, D. J. Gaussian, Inc., Wallingford CT, 2009.

(20) Marenich, A. V. ; Cramer, C. J.; Truhlar, D. G. Universal Solvation Model Based on Solute Electron Density and on a Continuum Model of the Solvent Defined by the Bulk Dielectric Constant and Atomic Surface Tensions. *J. Phys. Chem. B*, **2009**, *113*, 6378-96.

(21) Beuermann, S.; Buback, M.; Davis, T. P.; Gilbert, R. G.; Hutchinson, R. A.; Olaj, O. F.; Russell, G. T.; Schweer, J.; van Herk, A. M. Critically Evaluated Rate Coefficients for Free-Radical Polymerization. 2. Propagation Rate Coefficients for Methyl Methacrylate. *Macromol. Chem. Phys.* **1997**, *198*, 1545-1560.

(22) Gridnev, A. A. ; Ittel, S. D. Dependence of Free-radical Propagation Rate Constants on the Degree of Polymerization. *Macromolecules* **1996**, *29*, 5864-5874.

(23) Lin, C. Y.; Coote, M. L.; Gennaro, A.; Matyjaszewski, K. Ab Initio Evaluation of the Thermodynamic and Electrochemical Properties of Alkyl Halides and Radicals and Their Mechanistic Implications for Atom Transfer Radical Polymerization. *J. Am. Chem. Soc.* **2008**, *130*, 12762-12774.

(24) Goto, A.; Terauchi, T.; Fukuda, T.; Miyamoto, T. Gel Permeation Chromatographic Determination of Activation Rate Constants in Nitroxide-controlled Free Radical Polymerization. 1. Direct Analysis by Peak Resolution. *Macromol. Rapid Commun.* **1997**, *18*, 673-681.

(25) Coessens, V.; Matyjaszewski, K. Synthesis of Polymers with Hydroxyl End Groups by Atom Transfer Radical Polymerization. *Macromol. Rapid Commun.***1999**, *20*, 127–134.

(26) Ishikawa, T. *Superbases for organic synthesis: Guanidines, Amidines, Phosphazenes and Related Organocatalysts*; John Wiley & Sons: London, UK, 2009.

For Table of Contents use only

Theoretical and Experimental Studies on Elementary Reactions in Living Radical Polymerization via Organic Amine Catalysis

Atsushi Goto, Shohei Sanada, Lin Lei, Kenji Hori**